Alkylamine Sensing Using Langmuir−Blodgett Films of *n*-Alkyl-*N*-phenylamide-Substituted Zinc Porphyrins

S. Brittle,[†] T. H. Richardson,*[,†] A. D. F. Dunbar,[†] S. Turega,[‡] and C. A. Hunter[‡]

Department of Physics and Astronomy, Hicks Building, University of Sheffield, Hounsfield Road, Sheffield S3 7RH, U.K., and Department of Chemistry, Dainton Building, University of Sheffield, Brook Hill, Sheffield S3 7HF, U.K.

Received: April 24, 2008; Revised Manuscript Received: June 12, 2008

Two porphyrin compounds, zinc(II) 5,10,15,20-tetrakis(3,5,5-trimethyl-*N*-phenylhexanamide)porphyrin and zinc(II) 5,10,15,20-tetrakis(2,2-dimethyl-*N*-phenylpropanamide)porphyrin, have been investigated as possible candidates for the detection of alkylamines. UV−visible spectroscopy has shown that their solution absorption spectra are significantly modified upon interaction with a range of organic analytes, including acetic acid, butanone, ethylacetate, hexanethiol, octanal, octanol, alkylamines, and trimethylphosphite. Large spectral changes are observed for the family of alkylamines as a result of the specific affinity between zinc and the amine moiety. Langmuir−Blodgett (LB) films of the porphyrins have been fabricated in order to assess their solid-state sensing capability toward amines. The surface pressure−area ($\Pi-A$) isotherms reveal a clear three-phase Langmuir film behavior and show that these monolayer films may be compressed to a relatively high surface pressure ($\sim$40−50 mN m^{-1}). The isotherm data alongside molecular modeling suggest a relatively flat orientation of the porphyrin rings of both compounds: that is, a mutually parallel alignment of the plane of the porphyrin ring and that of the water surface. LB films deposited at 15 mN m^{-1} have been exposed to alkylamine vapor (carried by N_2). A red shift and increase in intensity of the Soret band absorbance is observed which can be reversed by flowing pure N_2 over the gently heated sample (60 °C) after exposure. Primary amines were expected to invoke the greatest sensing response due to (i) their larger association constants with these porphyrins compared to secondary and tertiary amines and (ii) the ease of diffusion of amines which is expected to follow the order primary > secondary > tertiary due to the steric hindrance arising from the bulky secondary and tertiary amines. However, the magnitude of the absorbance change is largest for exposure to the secondary amines, dipropylamine and dibutylamine, for both porphyrins, compared to primary and tertiary amines. This trend follows that observed when the amines were added to solutions of the porphyrins. The rate of response of the porphyrin LB films falls as the molecular weight of the diffusing alkylamine increases. Furthermore, a greater rate of response is observed for the phenylhexanamide porphyrin compared to the phenylpropanamide porphyrin due to its lower molecular density within the LB film and therefore more porous structure.

Introduction

Porphyrin molecules possess highly conjugated π-electron systems which give rise to their characteristic UV−visible absorption spectra and hence their intense color.[1,2] Recently, they have been exploited as sensor materials for both inorganic[3] and organic[4] vapors since their spectra can be modified as a result of the binding interaction between the porphyrin ring and the analyte vapor molecule. To achieve a relatively fast response (approximately seconds), ultrathin films are required that offer a large surface area to volume ratio. The Langmuir−Blodgett technique[5,6] is an effective means of achieving this and is significantly faster than the commonly used layer-by-layer self-assembly methods.[7,8] In this work, two zinc substituted porphyrins, 5,10,15,20-tetrakis(3,5,5-trimethyl-*N*-phenylhexanamide)porphinatozinc(II) (**1**) and 5,10,15,20-tetrakis(2,2-dimethyl-*N*-phenylpropanamide)porphinatozinc(II) (**4**) were studied for potential use as amine sensing materials. The amine scent is very common and is found in odors from fish, rotting flesh, urine, and semen. Amine detection is of commercial interest because of toxicity and the potential health hazard to people working in the numerous industries which use amines. For example aliphatic amines are used in the production of dyes, emulsifiers, stabilizers, and corrosion inhibitors. The multiple amine content of some foods indicates its degree of spoilage, especially in fish and meats.[9]

Experimental Section

Materials. Compound **1** (Figure 1) and the corresponding *tert*-butyl derivative, **4**, used in this study were synthesized by coupling 5,10,15,20-tetrakis(3-aminophenyl)-21*H*,23*H*-porphyrin,[10] **2**, with isononyl chloride to provide porphyrin **5** in 50% yield and trimethylacetyl chloride to provide, 5,10,15,20-tetrakis(2,2-dimethyl-*N*-phenylpropanamide)-21*H*,23*H*-porphyrin, **3**, in 89% yield. Porphyrin **5** was then metalated with zinc acetate in 50% yield to give porphyrin **1**, and **3** was metalated to give zinc porphyrin, **4**, in 24% yield.

Synthesis. *5,10,15,20-Tetrakis(3,5,5-trimethyl-N-phenylhexanamide)-21H,23H-porphine,* 5. To a mixture of **2** (0.325 g, 0.482 mmol) and triethylamine (1.63 mL, 11.6 mmol) in tetrahydrofuran (THF, 20 mL) under nitrogen at room temper-

* To whom correspondence should be addressed. Phone/Fax: +44 114 2224280. E-mail: t.richardson@shef.ac.uk.
[†] Department of Physics and Astronomy.
[‡] Department of Chemistry.

10.1021/jp803577d CCC: $40.75
Published on Web 08/19/2008

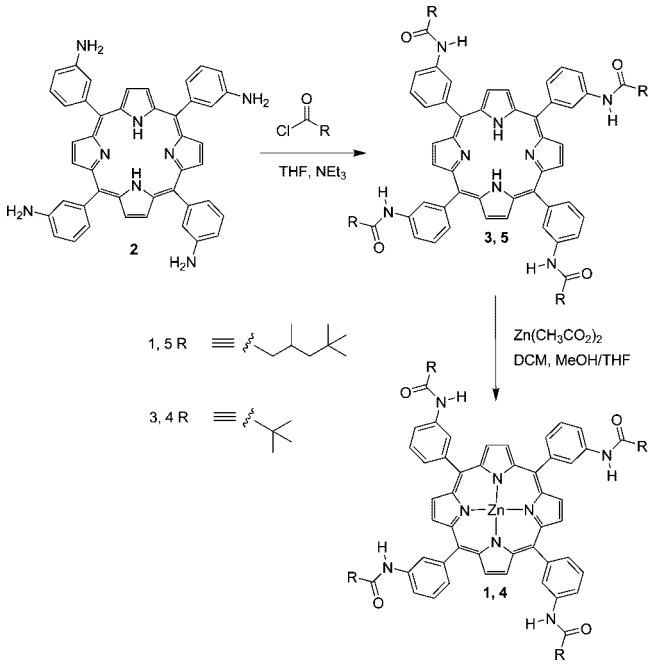

Figure 1. Synthetic route to zinc porphyrins **1** and **4**.

ature, isononanoyl chloride (0.366 mL, 1.93 mmol) was added, and the solution was stirred for 18 h. The solution was concentrated under reduced pressure and the resulting blue gum dessolved in DCM (250 mL), washed with 10% $NaHCO_2$ (aq), (2 × 200 mL), brine (200 mL), and condensed under reduced pressure. The crude product was purfied on silica (30 g) eluting with DCM−5% methanol. The product **5** was isolated as a purple colored solid, 0.297 g (50%). Mp = 250 °C (decomp.). ^{1}H NMR (250 MHz, CD_3SOCD_3): δ_H 10.25 (1H, s), 8.89 (2H, s), 8.50 (1H, d, J = 10), 8.08 (1H, s), 7.92 (1H, d, J = 8), 7.74 (1H, dd, J = 8, J = 8), 2.2−2.39 (2H, m), 2.19 (1H, s), 1.06−1.36 (2H, m), 0.98 (3H, d, J = 5), 0.88 (9H, s), −2.96 (0.5H, s). MS (El+): *m*/*z* (%) 675 (100), 1236 (10), [M + H$^+$]. HRMS (El+). Calcd for $C_{80}H_{99}N_8O_4$: 1235.7789. Found: 1235.7825. UV/vis (DMSO) [λ_{max} (nm) (ϵ (mol^{-1} cm^{-1}))] 423 (5.1 × 10^5), 516 (1.8 × 10^4), 551 (7.9 × 10^3), 590 (5.3 × 10^3), 645 (4.2 × 10^3).

***5,10,15,20-Tetrakis(2,2-dimethyl-N-phenylpropanamide)-21H,23H-porphyrin,* 3.** A mixture of **2** (0.200 g, 0.296 mmol) and triethylamine (0.360 g, 3.56 mmol) in 10:1 THF:DCM (250 mL) was stirred under nitrogen at room temperature. Trimethylacetyl chloride (0.146 mL, 1.19 mmol) was added, and the solution was stirred for 3 days. The precipitate was collected and washed 3 times with DCM (3 × 50 mL), giving **3**, which was isolated as a purple solid, 0.265 g (89%). Mp = 220 °C (decomp.). ^{1}H NMR (250 MHz, CD_3SOCD_3): δ_H 9.59 (1H, s), 8.91 (2H, s), 8.59 (1H, d, J = 6), 8.18 (1H, d, J = 8), 7.92 (1H, d, J = 8), 7.74 (1H, dd, J = 8, J = 8), 1.27 (9H, s), −2.94 (0.5H, s). ^{13}C NMR (100 MHz, CD_3SOCD_3): δ_C 177.4, 141.8, 138.5,130.0, 127.5, 126.8,120.4, 120.1, 27.7. MS (FAB+): *m*/*z* (%) 1011.6 (100) [M + H$^+$]. HRMS (FAB+). Calcd for $C_{64}H_{67}N_8O_4$: 1011.528528. Found: 1011.531530. UV/vis (DMSO) [λ_{max} (nm) (ϵ (mol^{-1} L cm^{-1}))] 423 (7.7 × 10^5), 516 (2.9 × 10^4), 550 (1.3 × 10^4), 591 (8.6 × 10^3), 647 (8.2 × 10^3).

***Zinc(II) 5,10,15,20-Tetrakis(3,5,5-trimethyl-N-phenylhexanamide)porphine,* 1.** A mixture of **5** (0.300 g, 0.243 mmol) and zinc acetate (0.890 g, 4.85 mmol) in chloroform (20 mL)/MeOH (30 mL) was stirred under nitrogen at room temperature for 1.5 h The solution was concentrated under reduced pressure, and the resulting blue gum was purfied on deactivated alumina (80 g) eluting with DCM. The product **1** was isolated as a purple colored solid, 0.159 g (50%). Mp = 195 °C (decomp.). ^{1}H NMR (250 MHz, $CDCl_3$, CD_3OD, 2%): δ_H 8.89 (2H, s), 8.76 (1H, s), 8.14−8.19 (1H, m), 7.86−8.00 (2H, m), 7.57 (1H, s), 2.28−2.38 (2H, m), 2.04−2.014 (1H, m), 1.02−1.28 (2H, m), 0.96 (3H, d, J = 5), 0.83 (9H, s). MS (El+): *m*/*z* (%) 1299 (100) [M$^+$]. HRMS (El+). Calcd for $C_{80}H_{96}N_8O_4{}^{64}Zn$: 1296.6846. Found: 1296.6835. UV/vis (DMSO) [λ_{max} (nm) (ϵ (mol^{-1} cm^{-1}))] 421 (4.6 × 10^5), 549 (1.6 × 10^4), 595 (4.7 × 10^3).

***Zinc(II) 5,10,15,20-Tetrakis(2,2-dimethyl-N-phenylpropanamide)porphyrin,* 4.** A mixture of **3** (0.200 g, 0.198 mmol) and zinc acetate (0.727 g, 3.96 mmol) in 95:5 THF:DCM (200 mL) was refluxed under nitrogen for 48 h. The solution was concentrated under reduced pressure, and the resulting blue gum was purified by column chromatography on deactivated alumina (60 g) eluting with DCM:MeOH 99:1. The product **4** was isolated as a purple solid, 0.052 g (24%). Mp = 250 °C (decomp.). ^{1}H NMR (250 MHz, $CDCl_3$, CD_3OD, 2%): δ_H 8.96 (1H, s), 8.94 (2H, s), 8.58 (1H, s), 8.20 (1H, d, J = 8), 7.94 (1H, d, J = 8), 7.71 (1H, dd, J = 6, J = 6), 1.27 (9H, s). ^{13}C NMR (100 MHz, CD_3SOCD_3): δ_C 176.6, 149.9, 143.6, 137.9, 131.6, 129.7, 126.5, 120.4, 118.9, 39.5, 26.9. MS (ES+): *m*/*z* (%) 1012 (30), 1074 (100) [M + H$^+$]. HRMS (ES+). Calcd for $C_{64}H_{65}N_8O_4{}^{64}Zn$: 1073.4420. Found: 1073.4425 [M + H$^+$]. UV/vis (DMSO) [λ_{max} (nm) (ϵ (mol^{-1} L cm^{-1}) 431 (1.9 × 10^5), 562 (4.9 × 10^4), 601 (2.7 × 10^3).

Experimental Methods. ***Solution UV−Visible Spectroscopy.*** UV−visible titrations were carried out by preparing a 10 mL sample of the porphyrin **1** at known concentration (1−10 μM) in spectroscopic grade toluene. A 2 mL aliquot of this solution was removed, and a UV−visible spectrum was recorded using a Peltier thermostat set at 298 K. A 2 mL solution of pyridine ligand (5−2000 μM) was prepared using the porphyrin solution so that the concentration of porphyrin remained constant throughout the titration. Aliquots of pyridine solution were added successively to the cell containing the porphyrin solution, and the UV−visible spectrum was recorded after each addition. Changes in absorbance for the Soret band of the porphyrin were fit to a 1:1 binding isotherm in Microsoft Excel to obtain the association constant. Each titration was repeated at least twice, and the experimental error is quoted as twice the standard deviation at a precision of one significant figure.

Solutions of each of the porphyrins were prepared using chloroform as the solvent. 2 mL quantities of each of these porphyrin solutions were placed in quartz cuvettes, and initial absorption spectra of the solutions were recorded using an Ocean Optics USB2000 spectrometer with a Mikropack Mini D2 UV−vis−IR light source. The absorbance spectra were recorded in the range of 350−680 nm with respect to a reference taken of chloroform. Subsequently, aliquots of 100 μL of the analyte to be investigated were added to the porphyrin solution which was then stirred. After each addition, the exposed absorption spectrum was recorded. This process was repeated for both zinc porphyrins with each of the nine different analytes. The absorbance spectrum of each analyte in chloroform was also recorded to confirm they are transparent in the wavelength range of interest.

Langmuir Isotherms. Chloroform solutions of **1** and **4** were produced to a concentration of ∼0.2 mg/mL. The porphyrin solution was added dropwise onto the subphase surface of a Nima Langmuir trough (Nima model 611), using a 250 μL Hamilton syringe. The subphase of pure water was supplied by an Elga Purelab water system, providing pure water with

TABLE 1: Principal Absorption Wavelengths and Molar Extinction Coefficients for 1 and 4

porphorin	parameter		
1	λ (nm)	424 (Soret)	551 (Q-band)
	ϵ (mol^{-1} L cm^{-1})	185615	11764
4	λ (nm)	424 (Soret)	551 (Q-band)
	ϵ (mol^{-1} L cm^{-1})	183254	13530

resistivity >15 MΩ cm. A sufficient time period (5−10 min) was allowed for the cholorform to evaporate from the subphase surface. The Teflon barriers of the Nima Langmuir trough were then closed slowly at a speed of 50 cm^2 min^{-1} in order to compress the floating porphyrin Langmuir film. The surface pressure was measured during the compression using a Wilhelmy plate (filter paper) and monitored using Nima software. The area per molecule was plotted against surface pressure to obtain the Langmuir isotherm.

LB Film Fabrication. To produce LB films of **1** and **4**, a Langmuir layer was prepared in the same way as described above. The barriers of the Nima trough were then closed until the desired deposition pressure was obtained; this surface pressure was then maintained using the Langmuir trough feedback mechanism. The zinc porphyrin was then transferred onto a clean, hydrophobic (via silanization), glass substrate using the LB technique using a deposition arm speed of 10 mm min^{-1} and a surface pressure of 15 mN m^{-1}. Samples consisting of 20 Langmuir layers were produced.

Vapor Delivery. LB films of **1** and **4** were exposed to amine vapors using a specially designed gas testing chamber comprising two Tylan FC-260 mass flow controllers, which deliver a mixture of N_2 and amine vapor for the exposure stage, followed by pure N_2 for the recovery stage. The delivery of these gases was controlled and automated using a program developed using Labview software. The liquid amine bottled samples were kept in iced water during exposure. N_2 flowed over the surface of the amine liquid, transporting the gas mixture to the sample chamber. The LB film samples were positioned on a Peltier heating device containing an aperture in its center to allow transmission UV−visible spectroscopy to be conducted in situ. The Peltier heater was used to heat the films to 60 °C in order to accelerate desorption and hence allow the films to recover. LB film spectra over the range of 350−850 nm (tungsten light source) were monitored continually during exposure and recovery using a World Precision Instruments "Spectromate" spectrometer.

Results and Discussion

Table 1 shows the principal absorption wavelengths and extinction coefficients for solutions (chloroform solvent) of **1** and **4**. The very similar values confirm that the alkyl chain of the amide group plays little or no role in determining the oscillator strength of the porphyrin transitions. The addition of analytes (in liquid form) to porphyrins in solution offers an insight into the interaction between the nonaggregated, discrete porphyrin molecule and the analyte species to be bound.

Figure 2 shows the difference spectra of a chloroform solution of **1** for the range of nine analytes. Each difference spectrum is formed by subtracting the spectrum obtained prior to exposure to any analyte liquid from that measured after the addition of each analyte (saturation). Clearly, the response is unique for each analyte and is particularly strong (large absorbance change) for propylamine and octanol. Figure 3 shows the difference spectra corresponding to the exposure of a solution (chloroform) of **4** to the nine analytes. Comparison with Figure 2 reveals that the two porphyrins behave similarly.

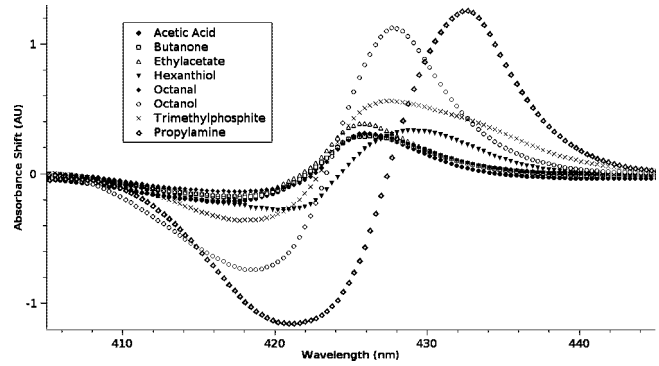

Figure 2. Difference spectra after the addition of several analytes to a chloroform solution of **1**.

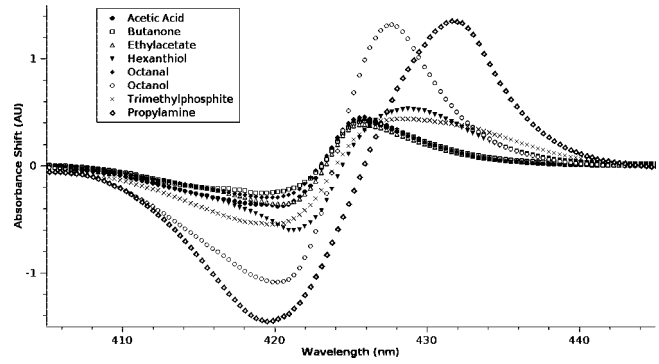

Figure 3. Difference spectra after the addition of several analytes to a chloroform solution of zinc porphyrin **4**.

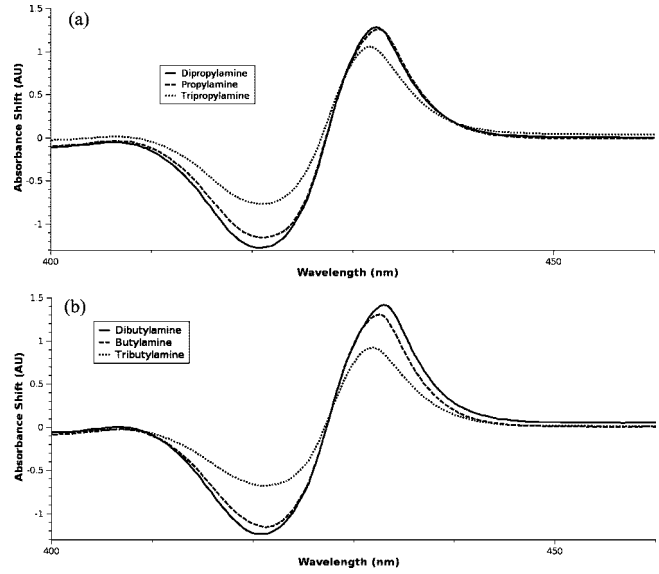

Figure 4. Difference spectra after the addition of alkylamines to a chloroform solution of porphyrin **1**: (a) effect of propylamine, dipropylamine, and tripropylamine, and (b) effect of butylamine, dibutylamin, and tributylamine.

Since amines have yielded the largest change in both zinc porphyrin spectra, their sensitivity in solution and solid state (LB films) was investigated using six alkylamines comprising two examples of primary, secondary, and tertiary amines. Figure 4 shows the difference spectra for the *n*-butylamines (Figure 4a) and the *n*-propylamines (Figure 4b) when added to a solution of porphyrin **1**. The largest absorbance change is observed for dibutylamine and dipropylamine.

The Langmuir isotherms of **1** and **4** are shown in Figure 5. Each isotherm clearly shows three separate phases.

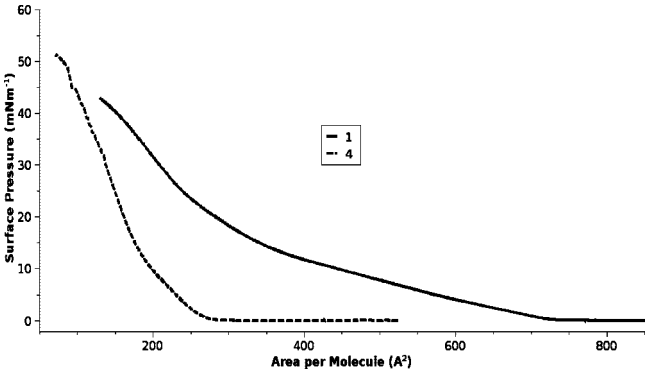

Figure 5. Surface pressure−area isotherms of **1** and **4**.

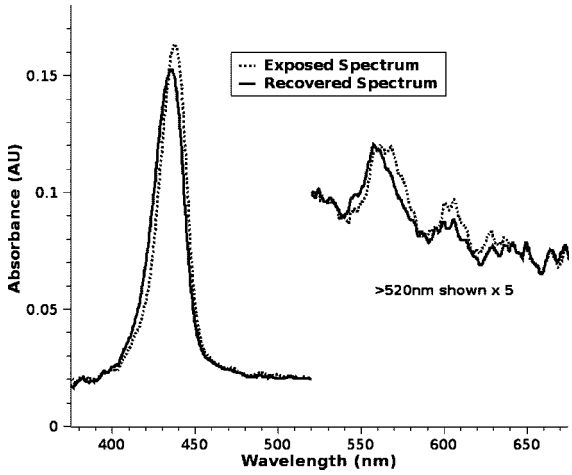

Figure 6. Spectra of 20 layer sample of **4** during exposure and recovery cycles to dipropylamine.

However, the takeoff area (the area per molecule at which the surface pressure Π becomes >0 mN m^{-1}) is significantly larger for **1** (730 ± 10 $Å^2$) compared to **4** (260 ± 10 $Å^2$). The middle of the three phases (liquid phase) is more expanded for **1** than **4**. Both of these differences are attributed to the length of the alkyl chain within the amide functional group, which is longer for **1** (hexanamide) than **4** (propanamide). The longer chain results in increased steric hindrance for the packing of molecules of **4** compared to **1**. At higher surface pressure, the solid phases are closer together for the two materials, although the area per molecule for **1** is appreciably larger (425 ± 20 $Å^2$ by extrapolation of the solid phase) than for **4** (240 ± 20 $Å^2$ by extrapolation). Corey−Pauling−Koltun (CPK) modeling indicates that molecules of **1** could indeed be oriented in a completely flat orientation (that is, the porphyrin ring could be oriented parallel to the plane of the water surface). The modeled cross-sectional area is 420 ± 40 $Å^2$, which is in close agreement with the measured value. The molecular orientation of **4** may be slightly tilted with respect to the water surface since the modeled value of 360 ± 30 $Å^2$ is slightly greater than the measured projected area per molecule on the water surface. An alternative interpretation may be that a small degree of aggregation between molecules of **4** exists within the Langmuir film.

Figure 6 shows the effect of dipropylamine vapor (carried by N_2) on a 20 layer LB film of **4**. Upon exposure, the Soret band absorbance at 434 nm shifts to 443 nm and its intensity increases by ∼10%; this is accompanied by a Q-band shift from 560 to 567 nm. Although these changes are very small, the World Precision Instruments spectrophotometer (Spectromate) is capable of monitoring such changes reliably.

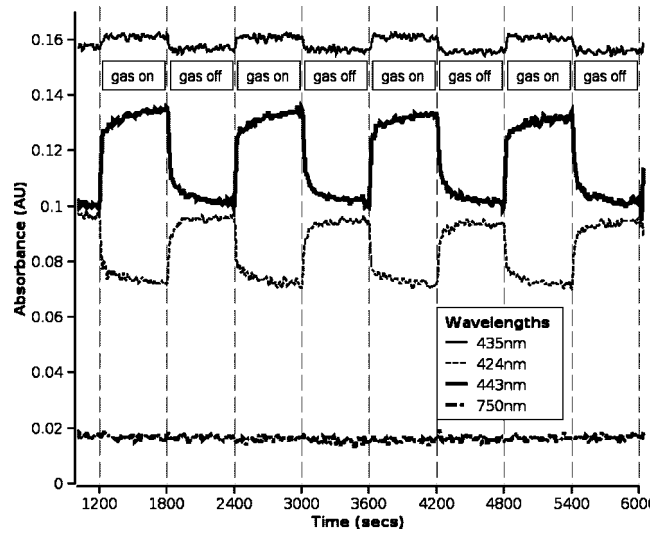

Figure 7. Absorbance dynamics for a 20 layer LB film of **4** upon exposure to dipropylamine.

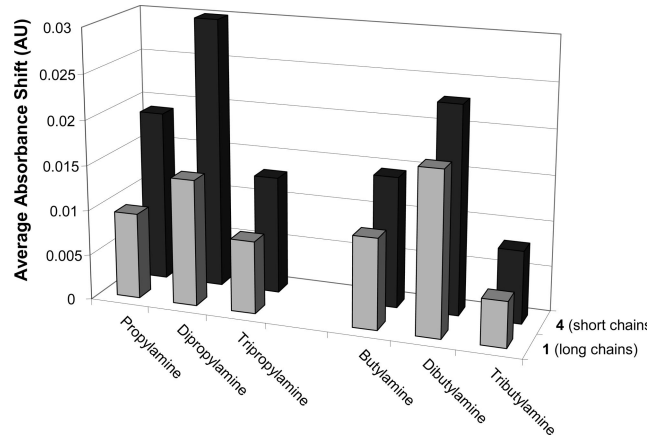

Figure 8. Histogram of the absorbance changes of the two porphyrin films when exposed to each of the six amine vapors.

The maximum absorption changes in the LB spectra of **1** and **4** occur not on the Soret band peak itself but on either side of this peak. By identifying the wavelength that changes the most during exposure to amine vapors, it is possible to maximize the signal response of the zinc porphyrin amine sensor and to monitor this signal as a function of time. The dipropylamine vapor is delivered to the sample for 600 s during a single exposure cycle, until a recovery stage in which clean nitrogen gas is delivered to the sample for a further 600 s. The four different wavelengths that are tracked in this case are the original Soret band (435 nm), the wavelengths for which maximum absorbance change is observed (424 and 443 nm), and a wavelength outside the absorption spectrum for reference purposes (750 nm).

Figure 7 shows the absorbance values at these four wavelengths plotted as a function of time. Upon exposure to the amine vapor, dramatic changes in absorbance are observed. At the Soret band (435 nm) a small increase in absorbance is detected, but at either side of the Soret band (424 or 443 nm), absorbance changes of around 20−30% are observed. It is clear from Figure 7 that the exposure− recovery cycle is reproducible and that, over the four complete cycles shown, little or no degradation in response is observed.

The plot in Figure 8 represents an example of the data collected by measuring the response of 20 layer LB films of each porphyrin to six different organic amines, namely, pro-

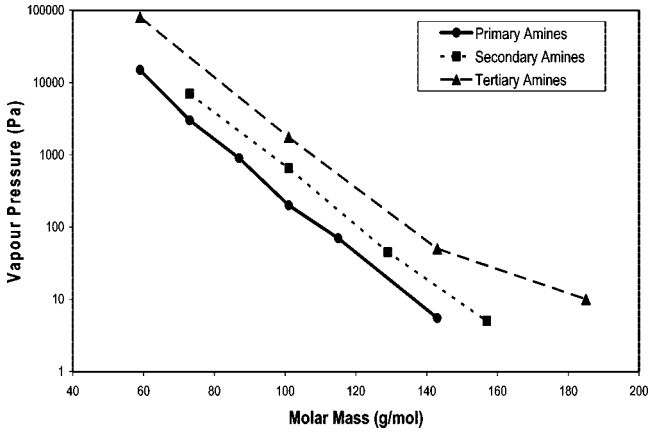

Figure 9. Vapor pressures (at 0 °C) for alkyl (methyl, propyl, and butyl) amines, dialkylamines, and trialkylamines.

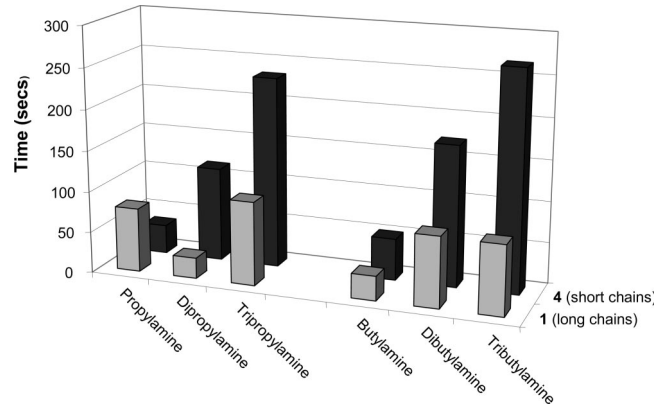

Figure 10. Histogram of the t_{90} value of the two porphyrin films when exposed to each of the six amine vapors.

pylamine, dipropylamine, tripropylamine, butylamine, dibutylamine, and tributylamine. These amines have been chosen since there are two examples of primary, secondary, and tertiary amines, and they are all volatile liquids at 0 °C, the temperature at which they are maintained prior to vapor delivery into the sample chamber. Figure 8 depicts the average absorbance change (over four response−recovery cycles) at 443 nm for the exposure of each porphyrin to each of the six amines.

The response of the 20 layer LB film of **4** is greater than that of film **1** for each corresponding amine. This is because the smaller area per molecule (Figure 5) of **4** compared to **1** means that the LB film of **4** possesses a higher molecular density and therefore a greater density of available active sites for interaction with amine molecules. The two *secondary amines*, dipropylamine and dibutylamine, induce a larger response, in both of the porphyrins, compared to the primary or tertiary amines. This trend agrees with the response measured in solution (Figure 4) and has been observed previously in a related system.[11] It was anticipated that primary amines would produce the greatest sensing response due to their larger solution binding constants with these porphyrins compared to secondary and tertiary amines. In this work, it was found that, for *tert*-butylamine, $K = 4100 \pm 100\ M^{-1}$; for diethylamine, $K = 810 \pm 100\ M^{-1}$; and for triethylamine, $K = 9.3 \pm 1.0\ M^{-1}$. However, the association constant is indicative of the fraction of binding pairs (porphyrin−amine) rather than the strength of the effect each bound amine has on the absorption spectrum. Our research data presented in Figure 4 and Figure 8 show that the secondary amines produce a larger absorbance change than primary or tertiary amines. We hypothesize that the binding of secondary amines by these porphyrins results in a strongly asymmetric porphyrin ring distortion compared to that resulting from the binding of tertiary amines. Primary amines are expected also to induce an asymmetric ring distortion, but this will be less pronounced than for secondary amines as a result of the presence of only one alkyl group (primary) rather than two in secondary amines.

Additionally, it must be noted that the liquid amines are held at 0 °C prior to delivery into the sample chamber. Since their vapor pressures are different, the concentrations delivered to the test chamber will not be the same. Figure 9 shows the vapor pressures for a series of primary, secondary, and tertiary amines including some of those tested here. The vapor pressures for the propylamine series follows the trend propylamine (molecular weight, MW = 59) > dipropylamine (MW = 101) > tripropylamine (MW = 143), and that for the butylamine series follows the trend butylamine (MW = 73) > dibutylamine (MW = 129) > tributylamine (MW = 185). Thus, if concentration were the dominating factor in determining the sensor response, the primary amines would be expected to show by far the greatest response.

The ease of diffusion of amines through a relatively dense LB matrix is expected to follow the order primary > secondary > tertiary due to the steric hindrance arising from the bulky secondary and tertiary amines. The time taken for 90% of the total change in absorbance (saturation) to occur is known as t_{90} and is a parameter often used in the sensor community to quantify the response rate. The t_{90} values, shown in Figure 10, indicate that the rate of response is diffusion-limited and the time taken for a porphyrin−amine binding pair to form increases as the molecular weight of the amine increases. This relation is not linear but empirically follows a trend in which $t_{90} = bM^{\sim 1.4-1.8}$ in which b is a constant and M is the molecular weight of the diffusing amine molecule.[12] Figure 10 also shows that the t_{90} value is greater for amine diffusion through **4** than **1**. The lower area per molecule of **4** compared to **1** results in an LB matrix through which diffusion would be expected to be more difficult due to the increased molecular density. The only exception to this trend is for the diffusion of propylamine through **1**, which takes longer than expected to react.

Conclusions

Electronic spectroscopy has shown that the UV−visible absorption spectra of two porphyrin compounds, zinc(II) 5,10,15,20-tetrakis(3,5,5-trimethyl-*N*-phenylhexanamide)porphyrin and zinc(II) 5,10,15,20-tetrakis(2,2-dimethyl-*N*-phenylpropanamide)-porphyrin, are significantly modified when exposed to a range of organic analytes including acetic acid, butanone, ethylacetate, hexanethiol, octanal, octanol, alkylamines, and trimethylphosphite. In this work, their large spectral response to a family of alkylamines, which occurs due to the specific affinity between zinc and the amine moiety, has been investigated. The addition of *n*-butylamines and *n*-propylamines to solutions of **1** results in the greatest absorbance changes occurring for the two secondary amines, dipropylamine and dibutylamine. Surface pressure−area isotherms yield a clear three-phase Langmuir film behavior and show that these floating films may be compressed to a relatively high surface pressure (~40−50 mN m^{-1}). A red shift and decrease in intensity of the Soret band absorbance is observed during exposure of LB films of porphyrins **1** and **4** to alkylamine vapor (carried by N_2) which is completely reversible. The greatest absorbance change occurs for both porphyrins (in both solution and solid states) during exposure to the secondary

amines, dipropylamine and dibutylamine, compared to primary and tertiary amines. This is an unexpected result since primary amines exhibit the largest association constants when compared to secondary and tertiary amines and are also expected to diffuse more rapidly through an organic matrix. The t_{90} value (the time taken for 90% of the total change in absorbance (saturation) to occur) of the porphyrin LB films increases as the molecular weight of the diffusing alkylamine increases. Moreover, higher response rates are observed for the phenylhexanamide porphyrin than the phenylpropanamide porphyrin because of its lower molecular density within the LB film and therefore more porous structure. Future work will focus on investigating the dependence on the optical response of porphyrin LB films to different concentrations of secondary amines in order to determine the detection limit and saturation point of these materials.

Acknowledgment. The authors of this paper thank the EPSRC for the financial support they have provided to support this research (Grant GR/S96845/01). We also thank William Barford for useful discussion.

References and Notes

(1) Milgrom, L. R. *The colours of life*; Oxford University Press: Oxford, U.K., 1997.
(2) Hunter, C. A.; Tregonning, R. *Tetrahedron* **2002**, *58* (4), 691–697.
(3) Richardson, T. H.; Dooling, C. M.; Jones, L. T.; Brook, R. A. *Adv. Colloid Interface Sci.* **2005**, *116*, 81–96.
(4) Dunbar, A. D. F.; Richardson, T. H.; McNaughton, A. J.; Hutchinson, J.; Hunter, C. A. *J. Phys. Chem. B* **2006**, *110*, 16646–16651.
(5) Petty, M. C. *Molecular Electronics*; John Wiley & Sons: Chichester, U.K., 2007.
(6) Roberts, G. G. *Langmuir-Blodgett Films*; Plenum Press: New York, 1990.
(7) Cassier, T.; Lowack, K.; Decher, G. *Supramol. Sci.* **1998**, *5*, 309–315.
(8) Freeman, T. L.; Evans, S. D.; Ulman, A. *Langmuir* **1995**, *11*, 4411–4417.
(9) Lawrence, S. A. *Amines*; Cambridge University Press: Cambridge, U.K., 2004.
(10) Semeikin, A. S.; Koifman, O. I.; Berezin, B. D. *Izv. Vyssh. Uchebn. Zaved., Khim. Khim. Tekhnol.* **1985**, *28* (11), 47–51.
(11) Brittle, S.; Richardson, T. H.; Hutchinson, J.; Hunter, C. A. *Colloids Surf., A*, in press (doi: 10.1016/j.colsurfa.2008.02.042.
(12) Jones, R. A. L. *Soft Condensed Matter*; Oxford University Press: Oxford, U.K., 2002.

JP803577D